JTERA (Jurnal Teknologi Rekayasa), Vol. 10, No. 2, Desember 2025, Hal. 181-190 p-ISSN 2548-737X
Terakreditasi "**Peringkat 3**" oleh Kemdiktisaintek, Nomor : 10/C/C3/DT.05.00/2025 e-ISSN 2548-8678
DOI: 10.31544/jtera.v10.i2.2025.181-190

The Effect of The Bio-Inspired Airfoil NACA 4415 at High Reynolds Number

Saphira Anggraita Siswanto[1], James Julian[1], Fitri Wahyuni[1], Riki Hendra Purba[1], Fathin Muhammad Mahdhudhu[2], Elvi Armadani[3]
[1]Departement of Mechanical Engineering, Universitas Pembangunan Nasional Veteran Jakarta
[2]Departement of Naval Architecture, Universitas Pembangunan Nasional Veteran Jakarta
[3]Departement of Industrial Engineering, Universitas Pembangunan Nasional Veteran Jakarta
Jl. Rs. Fatmawati, Pondok Labu, Kota Jakarta Selatan 12450, Indonesia
zames@upnvj.ac.id

Abstrak

Topik modifikasi airfoil dan dampaknya terhadap kinerja aerodinamis merupakan isu yang sangat diperdebatkan di kalangan teknik kedirgantaraan. Studi ini mengkaji pengaruh airfoil hidung bio-inspired NACA 4415 terhadap kinerja aerodinamisnya dengan menambahkan geometri spinner dolphin dan roughtoothed dolphin ke tepi depan menggunakan metode Computational Fluid Dynamics (CFD) pada bilangan Reynolds Re = 10^6. Simulasi dilakukan untuk menganalisis perubahan koefisien gaya angkat (Cl), koefisien gaya hambat (Cd), dan koefisien momen (Cm), yang berfungsi sebagai indikator kinerja dan stabilitas aerodinamis. Hasil penelitian menunjukkan bahwa airfoil NACA 4415 dasar menghasilkan gaya angkat tertinggi dan gaya hambat terendah secara keseluruhan, sehingga cocok untuk aplikasi yang membutuhkan gaya angkat maksimum dan gaya hambat minimum. *Spinner dolphin* memiliki persentase peningkatan Cd yang lebih kecil, yaitu 41,933%, dibandingkan dengan dasar. Sebaliknya, *Roughtoothed dolphin* dengan persentase rata-rata 56,004% dibandingkan dengan data dasar menunjukkan peningkatan persentase Cd yang lebih tinggi. Sebaliknya, pada data Cl, persentase penurunan pada *Roughtoothed dolphin* memiliki rata-rata yang lebih besar, yaitu -14,607%, dibandingkan dengan data dasar, sedangkan jenis *Spinner dolphin* hanya memiliki rata-rata -8,713%. Pada data Cm, *Roughtoothed dolphin* dan *Spinner dolphin* memiliki Cm yang lebih tinggi dan lebih stabil daripada NACA 4415. Studi ini menegaskan bahwa modifikasi yang terinspirasi oleh biologi dapat berdampak signifikan pada kinerja aerodinamis, tergantung pada kondisi operasi.

Kata kunci: profil sayap, terinspirasi dari alam, dinamika fluida komputasional, parameter tak berdimensi, NACA 4415

Abstract

The topic of airfoil modification and its impact on aerodynamic performance is a highly debated issue in aerospace engineering circles. This study examines the effect of the NACA 4415 bio-inspired nose airfoil on its aerodynamic performance by adding spinner dolphin and roughtoothed dolphin geometries to the leading edge using the Computational Fluid Dynamics (CFD) method at a Reynolds number of Re = 10^6. Simulations were conducted to analyze changes in the lift coefficient (Cl), drag coefficient (Cd), and moment coefficient (Cm), which serve as indicators of aerodynamic performance and stability. The results show that the baseline NACA 4415 airfoil produces the highest lift and the lowest drag overall, making it suitable for applications requiring maximum lift and minimum drag. Spinner dolphins has a smaller percentage increase in Cd, at 41.933%, compared to the baseline. In contrast, roughtoothed dolphins with an average percentage of 56.004% compared to the baseline exhibit a higher percentage increase in Cd. Conversely, in the Cl data, the percentage decreased in dolphins has a larger average, namely -14.607%, compared to the baseline, whereas the spinner dolphin type only has an average of -8.713%. In the Cm data, the Roughtoothed Dolphin and Spinner Dolphin have higher and more stable Cm than NACA 4415. This study confirms that bio-inspired modifications can significantly impact aerodynamic performance, depending on operating conditions.

Keywords: *airfoil, bio-inspired, CFD, nondimensional parameter, NACA 4415*

I. INTRODUCTION

Since ancient times, humans have been nomadic creatures, moving from one place to another. As time passes, humans strive to develop means of transportation that facilitate movement. In urban areas, transportation issues have become a recurring topic of interest [1]. According to its type, the means of transportation itself is divided into 3, the first is land transportation. Currently, researchers are intensively developing automobiles, from electric cars to self-driving cars [2], [3]. The second means of transportation is sea transportation; humans are competing to develop stable ships to sail on the open sea[4]. Moreover, air transportation is an interesting topic to discuss, as it is a type of transportation that requires the shortest time compared to the other two types of transportation. For this reason, numerous studies have been conducted to research airplanes[5], [6]. One important part that affects aircraft performance is airfoil design [7]. To create an airfoil with optimal aerodynamics, researchers are competing to develop new airfoil modifications.

Regarding airfoil modification and its impact on aerodynamic performance is a hot topic in aerospace engineering circles. Rubiat et al. conducted an experimental test on the NACA 4415 airfoil by adding hexagonal dimples to its side; the results of this modification indicate that it can inhibit stall [8]. Khurana and Kahl developed a study with a wing on a corrugated plate at Re = 34,000. The study concluded that the corrugated surface on the baseline limits aerodynamic efficiency at low Angle of Attack (AoA) on a flat plate [9]. Liu et al. modified the S814 airfoil by adding zigzags to the trailing edge, incorporating slotted airfoils, and combining the two methods. The results showed that adding zigzags on the trailing edge can reduce the drag coefficient (cd) at low AoA. In addition, the use of slotted airfoils causes an increase in the lift coefficient (cl) and a decrease in cd at high AoA, while the combination method can reduce cd at low to high AoA and reduce cl [10]. Zhang et al. conducted experiments on a 2-dimensional airfoil model with sinusoidal protuberances on its leading edge. The experiment results showed that these sinusoidal protuberances effectively prevented stall and significantly improved the airfoil's aerodynamics in the poststall region ($16° < \alpha < 70°$). They achieved a maximum increase of 25.0% in the cl, 39.2% in the lift-to-drag ratio, and a maximum decrease of 20.0% in the cd [11].

Following the above study, the development of airfoil modifications continues to be pursued. To date, there has been no research discussing the modification of spinner dolphins and roughtoothed dolphins using $Re = 10^6$. In this study, the innovation involves conducting a computational test of the NACA 4415 airfoil with a bio-inspired nose modification on its leading edge. The Reynolds number used in this study is $Re = 10^6$. Additionally, the study examines changes in the performance of the lift (Cl) and drag (Cd) coefficients between the modified and unmodified NACA 4415 airfoil at the same angle of attack. The aim is to understand the impact of modifications and flow parameters on the aerodynamic characteristics of the airfoil.

II. RESEARCH METHODOLOGY

In this study, the NACA 4415 airfoil will be tested using the Computational Fluid Dynamics (CFD) method to analyze its fluid flow. An outline of this study can be seen in Figure 1. In Figure 1, it can be seen that the outline of this study includes three stages. The first stage is pre-processing. In the pre-processing stage, information is searched through literature studies and data preparation through geometric processes. The geometry used in this study is the NACA 4415 airfoil model. After that, the meshing process and boundary condition determination are performed. After that, it enters the processing stage, namely the solver and grid independence test. If the grid independence test process fails, the entire process will be repeated, starting from meshing. Then, the final step is post-processing. In this final stage, all data will be taken, which will then be analyzed and conclusions drawn.

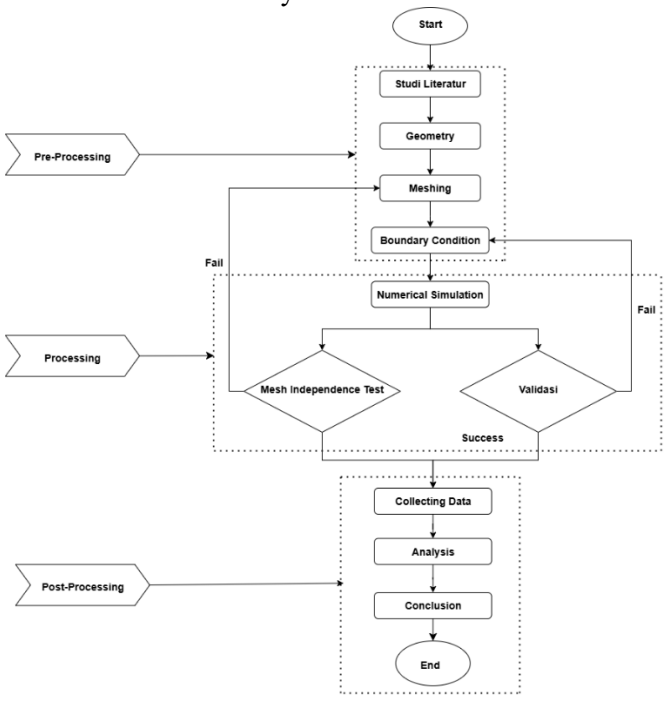

Figure 1. Flowchart

A. Airfoil Configuration

The NACA 4415 airfoil which can be seen in figure 2 is part of the 4-digit NACA series with a maximum camber of 4% at 40% chord length and a maximum thickness of 15% chord. This airfoil is known for its good aerodynamic performance, especially at certain angles of attack, with a high lift coefficient and stable response to changes in angle of attack and ground effects [12]. To improve aerodynamic efficiency, bio-inspired designs that mimic the wing surface structure of animals such as birds and marine mammals have begun to be implemented, which can optimize pressure distribution, resulting in greater lift and less drag [13].

In this study, simulations were performed on three airfoil geometries: the base NACA 4415, and two modifications with a bio-inspired approach, namely the spinner dolphin and roughtoothed dolphin shown in Figure 2, both modified at the leading edge with specific parameters such as cavity length, angle α, and radius R as shown in Table 1. Simulations were performed in a flow domain that accurately represents the flow boundary conditions to analyze the impact of modifications on the aerodynamic performance of the airfoil.

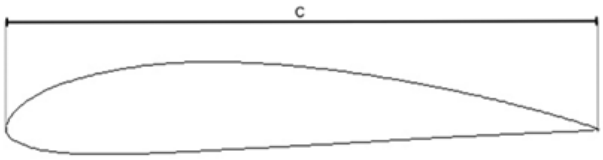

Figure 2. Airfoil NACA 4415

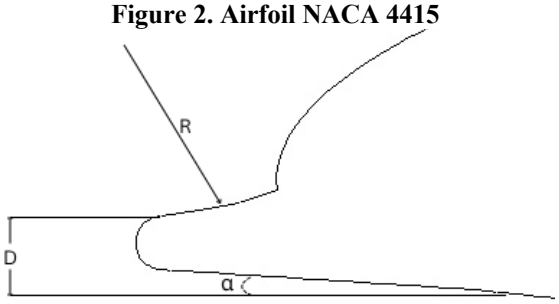

Figure 3. Airfoil Modification

Table 1. Airfoil Modification Spesification

	Spinner Dolphin	Roughtoothed Dolphin
D	20 mm	20 mm
R	68 mm	64,28 mm
α	5°	5°

B. Governing Equation

The governing equation used in this study refers to the Reynolds Averaged Navier Stokes (RANS). The RANS equation is a Navier-Stokes equation modified for CFD calculations. There are two constituting equations in the RANS equation: the continuity and momentum. The RANS calculation can be seen in equations 1 and 2 [14]. Equation 1 is the continuity equation, while Equation 2 is the momentum equation of the fluid flow. Meanwhile, equations 3, 4, and 5 represent the k-kl-ω turbulence model, representing the turbulent kinetic energy, laminar kinetic energy, and dissipation rate [15].

$$\frac{\partial \rho}{\partial t} + \frac{\partial}{\partial x_i}\left(\rho u_i\right) = 0 \tag{1}$$

ρ = the fluid density (kg/m^3)
t = time (s),
u = the velocity component (m/s),
x = the spatial coordinate (m).

$$\frac{\partial \rho}{\partial \tau}\left(\rho u_i\right) + \frac{\partial}{\partial x_i}\left(\rho u_i u_j\right) = \frac{\partial p}{\partial x_i}$$

$$+\frac{\partial}{\partial x_j}\left[\mu\left(\frac{\partial u_i}{\partial u_j} + \frac{\partial u_i}{\partial u_j} - \frac{2}{3}\delta_{ij}\frac{\partial u_i}{\partial u_i}\right)\right] \tag{2}$$

$$+\frac{\partial}{\partial u_i}\left(-\rho u'_i u'_j\right)$$

p = the static pressure (Pa),
μ = the dynamic viscosity of the fluid (Pa.s),
$u'_i u'_j$ = the Reynolds stress tensor representing turbulence effects.

$$\frac{\partial k}{\partial t} + u_j \frac{\partial k}{\partial x_j} = P_k - D_k \tag{3}$$

k = the turbulent kinetic energy (m^2/s^2),
P_k = the production term of the turbulent kinetic energy due to mean velocity gradients,
D_k = the dissipation term of turbulent kinetic energy.

$$\frac{\partial k_l}{\partial t} + u_j \frac{\partial k_l}{\partial x_j} = P_{kl} - D_{kl} \tag{4}$$

k_l = the laminar kinetic energy (m^2/s^2),
P_{kl} = the production term of the laminar kinetic energy due to mean velocity gradients,
D_{kl} = the dissipation term of laminar kinetic energy.

$$\frac{\partial \omega}{\partial t} + u_j \frac{\partial \omega}{\partial x_j} = P_\omega - D_\omega \tag{5}$$

ω = the specific dissipation rate (1/s),
P_ω = the production term of specific dissipation rate,
D_ω = the dissipation term of specific dissipation rate.

C. Mesh and Boundary Condition

The mesh is constructed using quadrilateral elements and a structured mesh scheme with local refinement around the airfoil shown in Figure 4(a). This mesh aims to accurately capture the boundary layer and flow transition region, with element spacing favoring low y^+ values as the transition turbulence model requires. The number of elements is adjusted through grid sensitivity testing to ensure the simulation results are free from the influence of mesh size. Boundary conditions include a velocity inlet with the velocity per the study, a zero gauge pressure outlet, the airfoil surface as a non-slip wall, and upper and lower boundaries as symmetry to minimize wall disturbances shown in Figure 4(b).

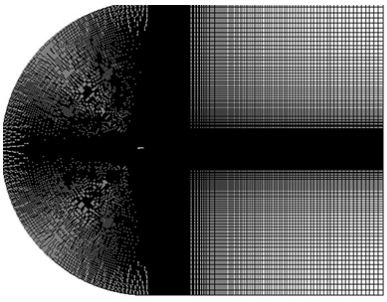

(a)

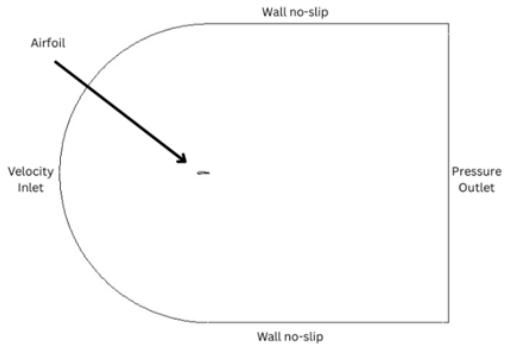

(b)

Figure 4. Mesh and Boundary Condition

D. Aerodynamic Parameters

In the discussion of airfoil aerodynamics, lift and drag are two forces that are never separated from the study of airfoil aerodynamics. An airfoil cannot function properly without the influence of these aerodynamic forces. The lift force has a vector perpendicular to the direction of the freestream flow and is the primary component that enables the airfoil to generate lift. Meanwhile, the drag force has a vector parallel to the direction of the freestream velocity. Meanwhile, the moment coefficient indicates the airfoil's tendency to rotate about a reference point due to the distribution of lift along its surface. A generally negative Cm value suggests a tendency for nose-down pitching moments, which are essential factors in maintaining the aerodynamic stability of a wing configuration or the aircraft as a whole. The calculation of the drag coefficient (Cd) and the lift coefficient (Cl) is mathematically shown in Equations (6) and (7) [16], and the moment coefficient is mathematically demonstrated in Equation (8)[17].

$$C_d = \frac{F_d}{\frac{1}{2}\rho V^2 c} \tag{6}$$

C_d = the drag coefficient,
F_d = the drag force acting on the airfoil (N),
V = the freestream velocity (m/s),
c = the airfoil Chord length.

$$C_l = \frac{F_l}{\frac{1}{2}\rho V^2 c} \tag{7}$$

C_l = the lift coefficient,
F_l = the lift force acting on the airfoil (N).

$$C_m = \frac{M}{\frac{1}{2}\rho V^2 c^2} \tag{8}$$

C_m = the pitching moment coefficient.
M = the aerodynamic pitching moment about the reference point (N.m).

E. Y-Plus (Y^+)

In CFD simulations, particularly in turbulent flows, the dimensionless parameter y^+ is used to measure the distance of the first cell from the wall to the flow boundary layer. The y^+ value is important to ensure accurate predictions near the wall, such as pressure distribution and friction forces. The ideal y^+ value varies depending on the turbulence model used. Using y^+ as a mesh verification approach is more efficient because it can improve local accuracy without increasing the overall number of elements, thus saving time and computational resources. The calculation of the y^+ value can be seen in equation (9) [18].

$$y^+ = \frac{\rho u_\tau y}{\mu} \quad (9)$$

y^+ = the dimensionless wall distance,
u_τ = the friction velocity (m/s),
y = the distance from the wall to the center of the first mesh cell (m),

Simulation verification of the NACA 4415 airfoil was performed to assess the reliability of the numerical model and the effect of mesh variations on the approximation of the experimental data. Three mesh types were used: fine (200,000 elements), medium (150,000 elements), and coarse (100,000 elements), all with quadrilateral elements and structured patterns to ensure quality around the airfoil surface shown in Figure 5. The y^+ value was carefully calculated, with the fine and medium meshes targeting around 1, while the coarse mesh was around 0.5 to improve the accuracy of the transition turbulence model. This approach helps to capture the boundary layer characteristics well.

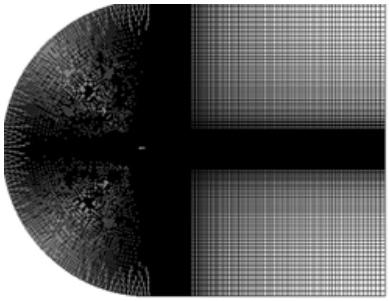

(a) Fine Mesh
200000 elements
y+ ≈ 1

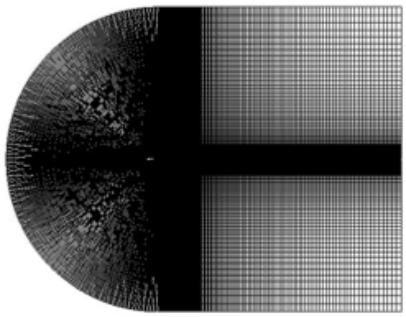

(b) Medium Mesh
150000 elements
y+ ≈ 1

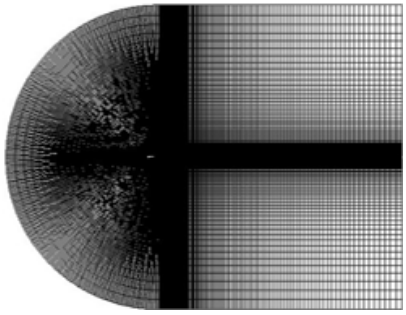

(c) Coarse Mesh
100000 elements
y+ ≈ 0.5

Figure 5. Mesh Types

Simulation results can be seen in Table 2 show that a coarse mesh with 100,000 elements provides the most accurate Cl and Cd results compared to fine and medium meshes, with relatively lower errors. This simulation indicates that a lower y^+ value in the coarse mesh positively affects accuracy, more than the number of mesh elements. This approach also reduces the computational burden because fewer mesh elements speed up simulation times.

Table 2. Simulation Results of y^+

k-kl-omega					
	Number of Elements	Cd		Cl	
Fine	200000	0.024217	19%	1.401135	-4%
Medium	150000	0.024227	19%	1.350139	2%
Coarse	100000	0.027884	7%	1.375177	-6%
Saliveros (1988)	eksperimen	0.03		1.3	

III. Results and Discussion

Validation

Before discussing the CFD simulation results, data validation is essential to ensure the accuracy of the data obtained. In this study, the NACA 4415 baseline computational data were compared with Hoffmann's NACA 4415 experimental data [19].The sample used was a NACA 4415 airfoil with Re = 10^6. Comparison of the drag (Cd) and lift (Cl) coefficient data from both samples is shown in Figure 6. The validation curves of the lift (Cl) and drag (Cd) coefficients illustrate the comparison of the experimental results with the NACA 4415 baseline as a function of the angle of attack (AoA). In the Cl graph, it can be seen that the experimental and baseline values rise to around AoA 13-15 before decreasing, indicating the stall point. Generally, the increasing trend is quite similar, although the experimental Cl is slightly lower after the stall. Meanwhile, in the Cd graph, both data also show an increase as AoA increases. However, the experimental Cd value tends to be slightly higher at medium to high AoA, which indicates that the drag in the experiment is slightly greater than the NACA 4415 baseline under these conditions.

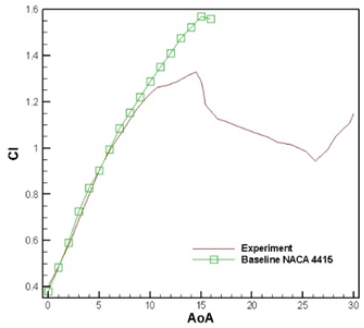

(a)

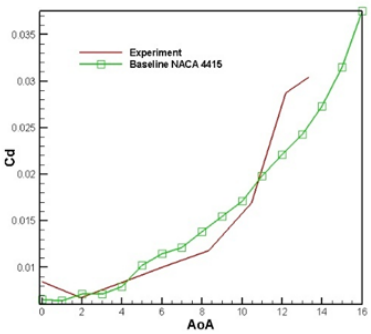

(b)

Figure 6. (a) Cl validation, (b) Cd validation against AoA

Data Analysis

This study uses a CFD data comparison method for three airfoil types. The three airfoil types being compared are the baseline NACA 4415 airfoil, the NACA 4415 airfoil with the spinner dolphin modification, and the NACA 4415 airfoil with the roughtoothed dolphin modification. The modifications made in this study involved adding geometry to the leading edge of the airfoils, representing the spinner dolphin and rough-toothed dolphin. All three airfoils were tested using a Reynolds number of Re = 10^6.

The primary data in this study are the lift coefficient (Cl) and drag coefficient (Cd), as shown in Figure 7. Figure 7(a) shows the relationship of Cl to angle of attack (AoA). The NACA 4415 appears to be the most efficient profile in producing high lift at almost all angles of attack. At low AoA, there is no significant difference in lift between the three airfoils. However, at medium AoA until stall, a significant difference begins to be seen between the three. Then, it can be seen that at the baseline, the NACA 4415 stall occurs at AoA 14 and the roughtoothed dolphin modification can maintain its stall also at the same AoA as the baseline. However, in the spinner dolphin modification, the stall occurs at AoA 12.

The drag coefficient (Cd) versus angle of attack (AoA) curve in Figure 7(b) shows that the Baseline NACA 4415 profile has the lowest drag at almost all angles of attack (AoA). At low AoA, there is no significant drag difference between the three airfoil types. However, as AoA increases, the drag increase of the roughtooth and spinner dolphin is more significant than that of the baseline NACA 4415. Significant differences begin to occur at AoA 7 and beyond.

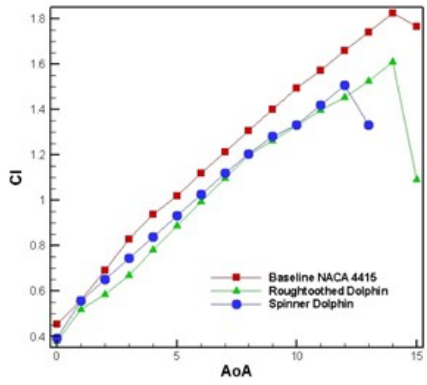

(a)

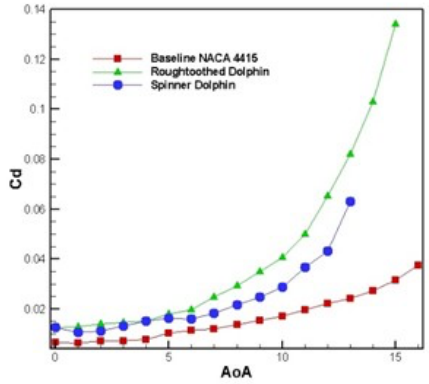

(b)

Figure 7. (a) Cl, (b) Cd against AoA

Figure 8 shows the graph of lift-to-drag ratio (Cl/Cd) against angle of attack (AoA) for three airfoils: the Baseline NACA 4415, the Roughtoothed Dolphin, and the Spinner Dolphin. The NACA 4415 airfoil has the best overall performance with the highest Cl/Cd values, especially at AoAs around 4-5°, indicating high aerodynamic efficiency, and is suitable for applications requiring maximum lift with minimum drag. With the addition of the roughtoothed dolphin and spinner dolphin modifications, it turns out to provide a decrease in the aerodynamics of the NACA 4415 airfoil, as can be seen from the lift-to-drag ratio curve which is much lower when compared to the baseline NACA 4415.

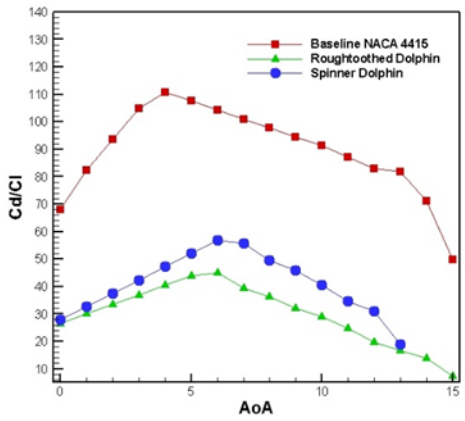

Figure 8. Graph lift-to-drag ratio against AoA

Cm data is presented to complement the existing data, which is used as a non-dimensional parameter to explain the airfoil stability shown in Figure 9. Pitch up occurs when Cm is positive (clockwise torque), while pitch down occurs when Cm is negative (counterclockwise torque). All Cm values are negative in the figure, indicating that the airfoil experiences a pitch-down motion. The airfoil is considered stable when the center of pressure (Cm) approaches zero. The curve results show that the Roughtoothed Dolphin and Spinner Dolphin have higher and more stable Cm than NACA 4415. Roughtoothed is superior at high angles of attack, Spinner is optimal at medium angles, while NACA 4415 is suitable for standard conditions but performs less well at extreme angles.

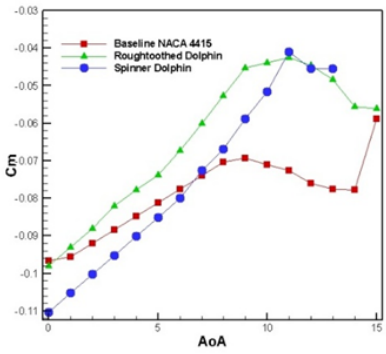

Figure 9. Graph Cm against AoA

To complement the above data, the average percentage data of cl and cd produced by additional modifications to the airfoil are presented. The Cl and Cd data shown in Table 3 are obtained by combining the Cl and Cd of the modified airfoil with the Cl and Cd of the baseline NACA 4415 airfoil. In the Cd data, it can be seen that the average percentage of spinner dolphins has a smaller percentage increase in Cd, at 41.933%, compared to the baseline. In contrast, roughtoothed dolphins with an average percentage of 56.004% compared to the baseline exhibit a higher percentage increase in Cd. Conversely, in the Cl data, the percentage decreased in roughtoothed dolphins has a larger average, namely -14.607%, compared to the baseline, whereas the spinner dolphin type only has an average of -8.713%.

Figure 10 presents the velocity contour, streamline velocity, and pressure contour data of the three airfoils taken at AoA 12. In the velocity contour, it can be seen that both modifications can increase the velocity on the upperside of the airfoil, while on the lower side, they reduce the velocity slightly. In streamlined velocity, there is no recirculation zone on the baseline airfoil. At the same time, there is a recirculation zone in both types of modifications, but the spinner dolphin type has a recirculation zone that tends to be smaller than that of the roughtoothed dolphin. While in the

pressure contour, it can be seen that both modifications are effective in reducing stagnation, and the roughtoothed dolphin type has the best performance among these three types of airfoils.

Table 3. Average percentage addition in Cd and Cl of modification roughtoothed and spinner dolphin

AoA	Cd		Cl	
	Roughtoothed Dolphin	Spinner Dolphin	Roughtoothed Dolphin	Spinner Dolphin
0	48.322%	47.784%	-12.651%	-8.692%
1	50.052%	39.132%	-4.932%	-2.323%
2	49.549%	36.052%	-13.376%	-1.975%
3	50.589%	45.592%	-22.165%	-9.880%
4	48.075%	48.187%	-19.496%	-11.175%
5	43.083%	37.841%	-14.809%	-9.204%
6	41.623%	28.537%	-12.524%	-9.000%
7	50.922%	33.211%	-11.360%	-9.124%
8	53.084%	36.091%	-8.262%	-7.968%
9	55.904%	37.842%	-8.834%	-7.355%
10	57.944%	40.355%	-9.351%	-9.039%
11	60.492%	46.239%	-8.816%	-7.242%
12	66.034%	48.689%	-9.498%	-5.538%
13	70.403%	61.511%	-8.936%	-28.114%
14	73.477%		-6.726%	
15	76.517%		-61.976%	
AVERAGE	56.004%	41.933%	-14.607%	-8.713%

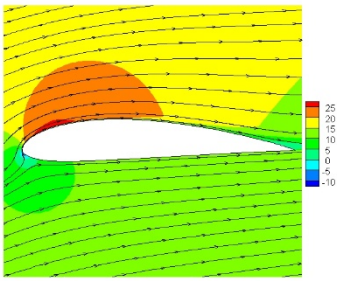

(a) velocity contour and streamline velocity of Baseline NACA 4415

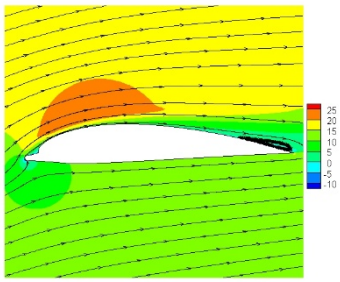

(b) velocity contour and streamline velocity of Roughtoothed Dolphin

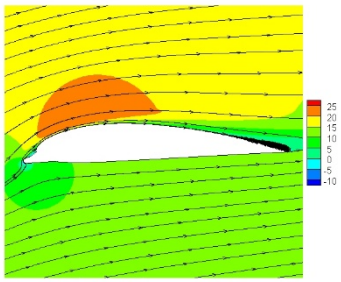

(c) velocity contour and streamline velocity of Spinner Dolphin

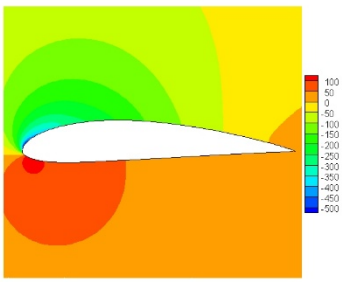

(d) pressure contour of Baseline NACA 4415

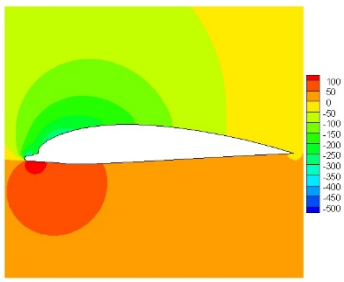

(e) pressure contour of Roughtoothed Dolphin

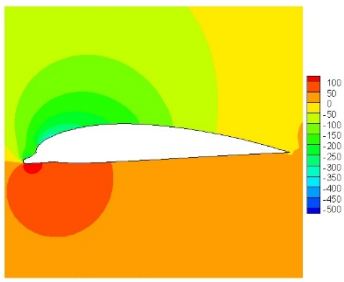

(f) pressure contour of Spinner Dolphin

Figure 10. Velocity contour, streamline velocity, and pressure contour at AoA 12

IV. Conclusion

The study results indicate that increasing the number of mesh elements does not always yield better results. By relying on the non-dimensional parameter method, a suitable mesh can be generated without requiring a mesh with a larger number of elements. The NACA 4415 baseline profile shows the best performance with the highest lift (Cl) across the entire AoA range, and the lowest drag coefficient (Cd) and the slowest increase to maximum AoA, making it very efficient for high lift and minimum drag requirements. However, both types of modifications effectively provide good stability at all AoAs. Therefore, it can be concluded that the spinner dolphin and roughtoothed dolphin modifications do not provide better aerodynamic effects than the baseline NACA 4415. However, both are effective in maintaining airfoil stability compared to the baseline NACA 4415.

REFERENCES

[1] G. P. Kurniawan, S. Zahra Shalikhah, H. Shofiati, N. N. Azizah, and M. Mochtar, "Analisis Permasalahan Transportasi di Perkotaan: Studi Kasus pada Kawasan Perkotaan Yogyakarta." [Online]. Available: https://ojs.staialfurqan.ac.id/jtm/index

[2] J. Y. Yong, V. K. Ramachandaramurthy, K. M. Tan, and N. Mithulananthan, "A review on the state-of-the-art technologies of electric vehicle, its impacts and prospects," *Renewable and Sustainable Energy Reviews*, vol. 49, pp. 365–385, 2015, doi: https://doi.org/10.1016/j.rser.2015.04.130.

[3] S. Sharma, "Fabricating an experimental setup to investigate the performance of an automobile car radiator by using aluminum/water nanofluid," *J Therm Anal Calorim*, vol. 133, no. 3, pp. 1387–1406, Sep. 2018, doi: 10.1007/s10973-018-7224-9.

[4] A. Hendrawan and A. M. Nusantara, "ANALISA INDIKATOR KESELAMATAN PELAYARAN PADA KAPAL NIAGA," 2019.

[5] S. Zelenika *et al.*, "Energy harvesting technologies for structural health monitoring of airplane components—a review," Nov. 02, 2020, *MDPI AG*. doi: 10.3390/s20226685.

[6] V. Madonna, P. Giangrande, and M. Galea, "Electrical Power Generation in Aircraft: Review, Challenges, and Opportunities," *IEEE Transactions on Transportation Electrification*, vol. 4, no. 3, pp. 646–659, Sep. 2018, doi: 10.1109/TTE.2018.2834142.

[7] P. R. Budarapu, Y. B. Sudhir Sastry, and R. Natarajan, "Design concepts of an aircraft wing: composite and morphing airfoil with auxetic structures," *Frontiers of Structural and Civil Engineering*, vol. 10, no. 4, pp. 394–408, Dec. 2016, doi: 10.1007/s11709-016-0352-z.

[8] R. Mustak, "Design and Construction of NACA-4415 Airfoil with Various Shaped Surface Modifications," 2017, doi: 10.20944/preprints201704.0124.v1.

[9] M. Khurana and J. Chahl, "Optimization of the leading edge segment of a corrugated wing," in *Bioinspiration, Biomimetics, and Bioreplication 2014*, A. Lakhtakia, Ed., SPIE, 2014, p. 905517. doi: 10.1117/12.2045031.

[10] L. Hongpeng, W. Yu, Y. Rujing, X. Peng, and W. Qing, "Influence of the modification of asymmetric trailing-edge thickness on the aerodynamic performance of a wind turbine airfoil," *Renew Energy*, vol. 147, pp. 1623–1631, 2020, doi: https://doi.org/10.1016/j.renene.2019.09.073.

[11] M. M. Zhang, G. F. Wang, and J. Z. Xu, "Aerodynamic control of low-reynolds-number airfoil with leading-edge protuberances," *AIAA Journal*, vol. 51, no. 8, pp. 1960–1971, Aug. 2013, doi: 10.2514/1.J052319.

[12] R. Saskia, R. Hayuningtyas, F. Fathori Nugroho, and B. Jalaali, "SIMULASI NUMERIK KARAKTERISTIK AERODINAMIKA PADA AIRFOIL NACA 4415 DENGAN MEMPERTIMBANGKAN GROUND EFFECT," 2023.

[13] A. Saputra, H. E. Priyono, I. Hidayat, L. Iryani, and D. M. Gunara, "MODIFIKASI AIRFOIL SAYAP PESAWAT CONCEPTUAL TRANSPORT RM-001," 2016.

[14] H. Xiao, J.-L. Wu, J.-X. Wang, R. Sun, and C. J. Roy, "Quantifying and reducing model-form uncertainties in Reynolds-averaged Navier–Stokes simulations: A data-driven, physics-informed Bayesian approach," *J Comput Phys*, vol. 324, pp. 115–136, 2016, doi: https://doi.org/10.1016/j.jcp.2016.07.038.

[15] D. K. Walters and J. H. Leylek, "A new model for boundary layer transition using a single-point RANS approach," *J Turbomach*, vol. 126, no. 1, pp. 193–202, Jan. 2004, doi: 10.1115/1.1622709.

[16] N. Alom, B. Borah, and U. K. Saha, "An insight into the drag and lift characteristics of modified Bach and Benesh profiles of Savonius rotor," *Energy Procedia*, vol. 144, pp. 50–56, 2018, doi: https://doi.org/10.1016/j.egypro.2018.06.007.

[17] S. Roy and A. Ducoin, "Unsteady analysis on the instantaneous forces and moment arms acting on a novel Savonius-style wind turbine," *Energy Convers Manag*, vol. 121, pp. 281–296, Aug. 2016, doi: 10.1016/j.enconman.2016.05.044.

[18] R. H. Nichols, "Turbulence Models and Their Application to Complex Flows," 2010.

[19] M. J. Hoffmann, R. Reuss Ramsay, and G. M. Gregorek, “Effects of grit roughness and pitch oscillations on the NACA 4415 airfoil,” United States, 1996. doi: 10.2172/266691.